

DEMIRS24787 Aileron East Airborne Magnetic and Radiometric Survey

Operations and Processing Summary Report

Contents

1 Survey Details	3
1.1 Survey Acquisition Summary	3
1.2 Survey Area	4
2 Aircraft	5
3 Personnel	6
4 Equipment Details	7
5 Magnetic Data Processing	14
6 Radiometric Data Processing	15
7 Elevation Data Processing	24
8 File Names	25
9 Data Format	27
10 Images of Grids	30
11 Quality Control Summary	31
12 References	36

1 Survey Details

Company Name	MAGSPEC Airborne Surveys Pty Ltd
Survey Name	Aileron East Airborne Magnetic and Radiometric Survey
Project Number	DEMIRS24787
Company Job Number	1436
Base of Operations	Kiwirrkurra, NT
Dates Flown	1 August 2025 – 15 December 2025

Block ID	Nominal Flying Height (m)	Flight Line Spacing (m) and Direction	Tie-Line Spacing and Direction	Flight, Tie and Repeat Numbering
1	50	100 / 000-180	1,000 / 090-270	Line numbering ABCCCD: - A = Block ID (1-9) B = Flightlines (0-8); Tielines (9) C = Line number (001-999) D = Repeat number (0-9)

1.1 Survey Acquisition Summary

The aircraft and crew were based in Kiwirrkurra, NT for the duration of the project, with periodic maintenance of the aircraft being conducted in Kununurra and Geraldton, WA. Two identically configured aircraft were employed, with rotation of crew on a scheduled basis.

Prior to production, an on-site safety meeting was completed by the crew, base stations were set up, reconnaissance, calibration and magnetic compensation flights were conducted, and radiometric test lines were established with sufficient separation between MAGSPEC aircraft and other operations to the west of the survey block.

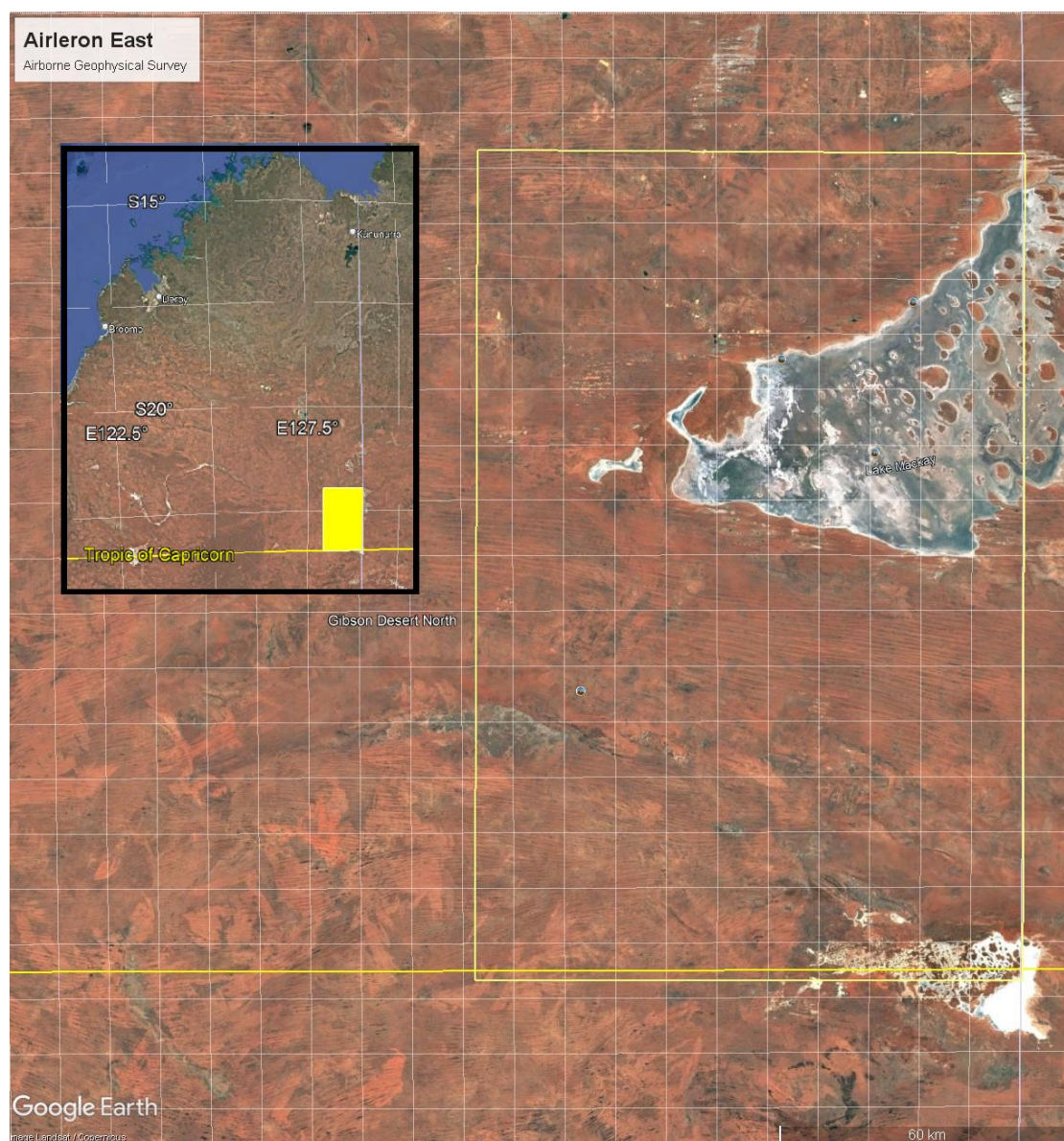
Production on the Aileron East Airborne Magnetic and Radiometric Survey began on 1st August 2025.

Weather conditions were varied throughout the survey period, overall being generally fine for flying, with some days of strong winds and storms restricting production. Magnetic diurnal activity varied from quiet to unsettled, with the occasional minor storm.

Data acquisition was completed on 15th December 2025, and the accumulated field data were checked; whereupon the aircraft and the field crew demobilised.

1.2 Survey Area

The Aileron East survey area is located on the border between WA and NT, as indicated in the figure below: -.



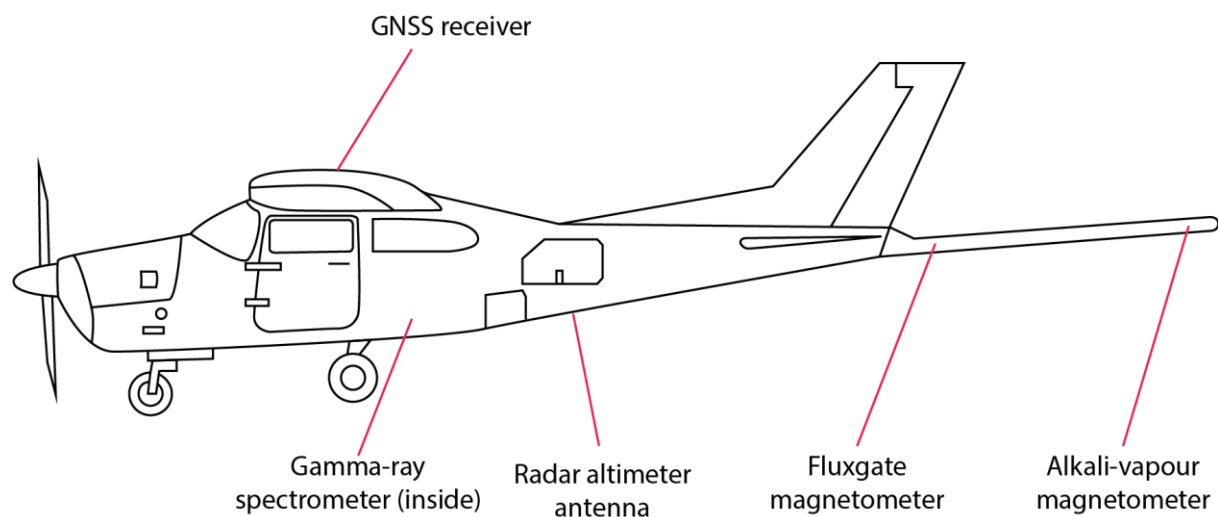
Survey Location (Google Earth)

MGA 52 Easting (m)	MGA 52 Northing (m)
500500	7404500
390000	7404500
390000	7570500
500500	7570500
500500	7404500

Boundary Extent Coordinates

2 Aircraft

Make and Model	Cessna 210M & Cessna 210L
Call Sign	VH-HHJ & VH-MDG
Base location(s) / Date	Kiwirrkurra, NT (Aug-Dec 2025)



Aircraft Configuration

3 Personnel

The following personnel were engaged for the project: -

Name	Position
Roger Spinks	Survey Pilot
Eiran Cooper	Survey Pilot
Daniel Wright	Survey Pilot
David Hart	Survey Pilot
George Robinson	Survey Pilot
Patrick Mudd	Survey Pilot
Hannah Longuet-Higgins	Survey Pilot
Louise Frank	Survey Pilot
David Saunders	Operator
Bailey Johnston	Operator
Andrew Taylor	Quality Control / Technical Support
Linsey Hale	Project Manager
Cameron Johnston	Data Processing Manager
Michael Lees	Sales Manager

4 Equipment Details

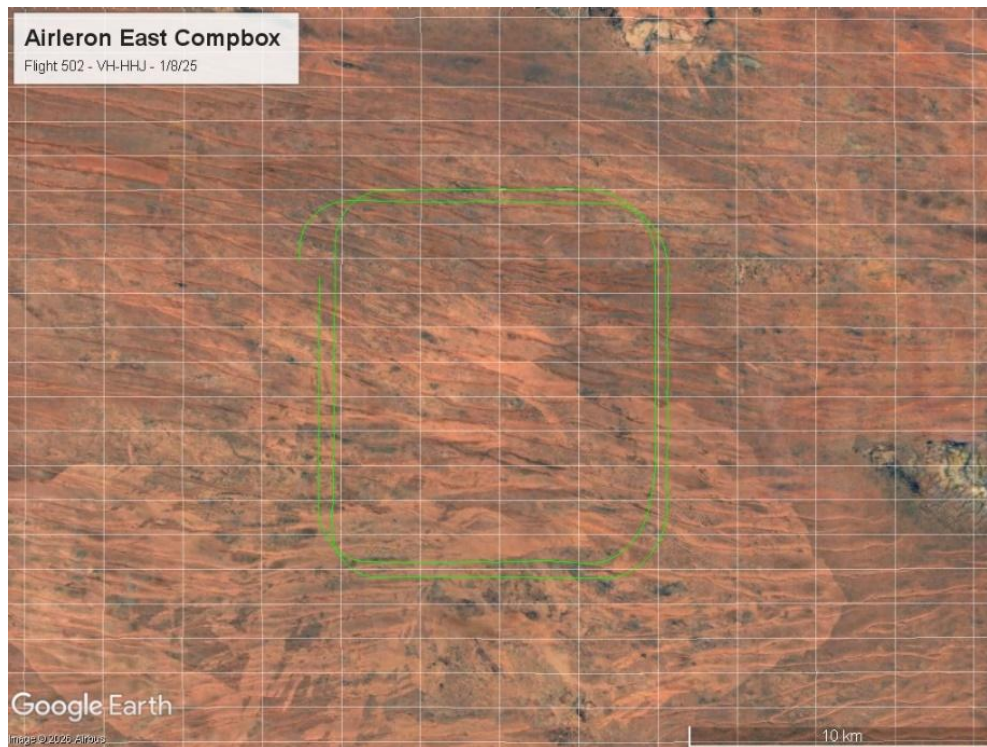
Acquisition System	Make and Model	GeoResults ZDAS DX2
	Fiducial Precision	0.05 sec
Electrical Current Meter	Current meter in use?	Yes
Global Navigation Satellite System (GNSS)	Make and Model	Novatel OEM719
	Sampling Rate (Hz)	2
	Horizontal Accuracy (cm)	40
	Vertical Accuracy (cm)	40
	Satellite Based Augmentation System (SBAS) in use?	Yes
	Dual frequency and/or carrier phase in use?	Yes
	Signal to noise ratio	45-50
Radar Altimeter	Make and Model	Honeywell KRA405B ZG
	Sampling Rate (Hz)	20
	Operating Range (m)	0-762
	Accuracy (%)	< 500ft $\pm 3\%$, >500ft $\pm 5\%$
	Precision (cm)	10
Barometer/Temperature Sensor	Make and Model	Setra 276
	Sampling Rate (Hz)	20
	Air Pressure Precision (%)	± 0.25
	Temperature Precision ($^{\circ}\text{C}$)	0.1
Total Field Magnetometer	Make and Model	Geometrics G822a
	Type (e.g. caesium vapour)	Caesium Vapour
	Sampling Rate (Hz)	20
	Sensitivity at Sampling Rate (nT)	$0.004/\sqrt{\text{Hz}}$
	Resolution (nT)	0.001
	Absolute Accuracy (nT)	< 3
	Dynamic Range (nT)	20,000 – 100,000
	50 Hz filter in use?	No
Three-Component Fluxgate Magnetometer	Make and Model	Billingsley TFM100G2
	Sampling Rate (Hz)	20
	Sensitivity at Sampling Rate (nT)	$100\mu\text{V/nT}$
	Resolution (nT)	0.01

	Absolute Accuracy (nT)	±0.5% of full scale
	Dynamic Range (nT)	±100,000
Base Station Magnetometer	Make and Model	GEM GSM-19
	Type	Overhauser
	Sampling Rate (Hz)	1
	Sensitivity at Sampling Rate (nT)	0.022
	Resolution (nT)	0.01
	Absolute Accuracy (nT)	0.1
	Dynamic Range (nT)	20,000 – 120,000
Gamma-Ray Spectrometer	Make and Model	Radiation Solutions Inc. RS-500
	Detector Geometry (e.g. tabular/12 crystals in 3 x 4 configuration)	Tabular/4x crystals per pack
	Integration Interval (seconds)	1.0 or 0.5
	No. Channels	1024 (256 recorded)
	Energy Range (keV)	0-3,000
	Downward Detector Volume (L)	32 (2x 16)
	Live Time Accuracy (%)	99.5 ("zero" dead time)
	Overall System Resolution (%)	<5.0
	Self-Stabilising?	Yes

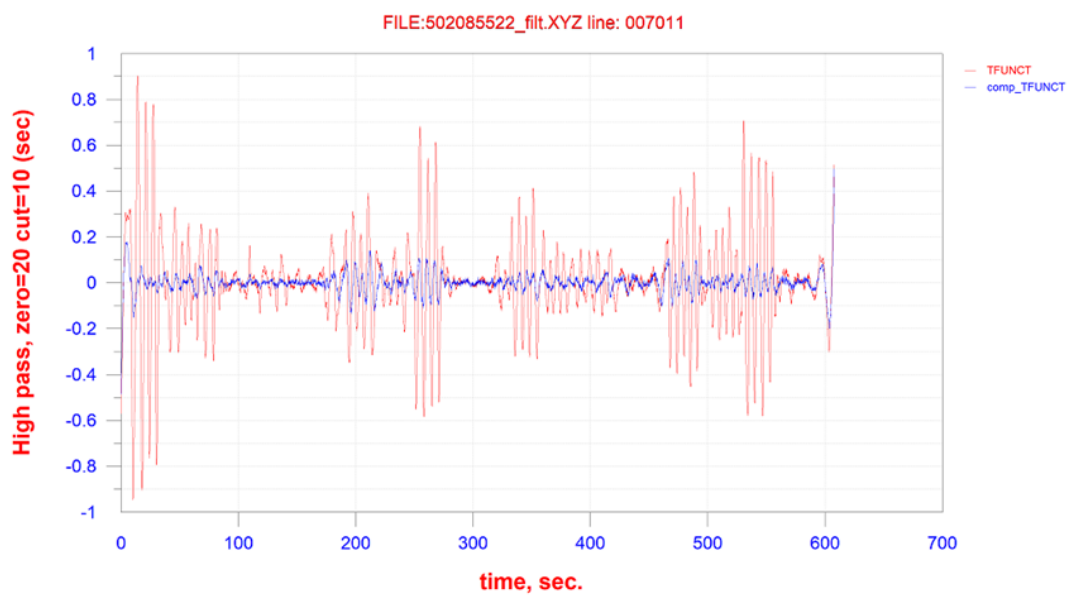
Magnetometer Compensation

Magnetic compensation flights (“compboxes”) were conducted at height, over an area of low magnetic gradient.

Magnetic Compensation Flight 502 (VH-HHJ) - 1st August 2025

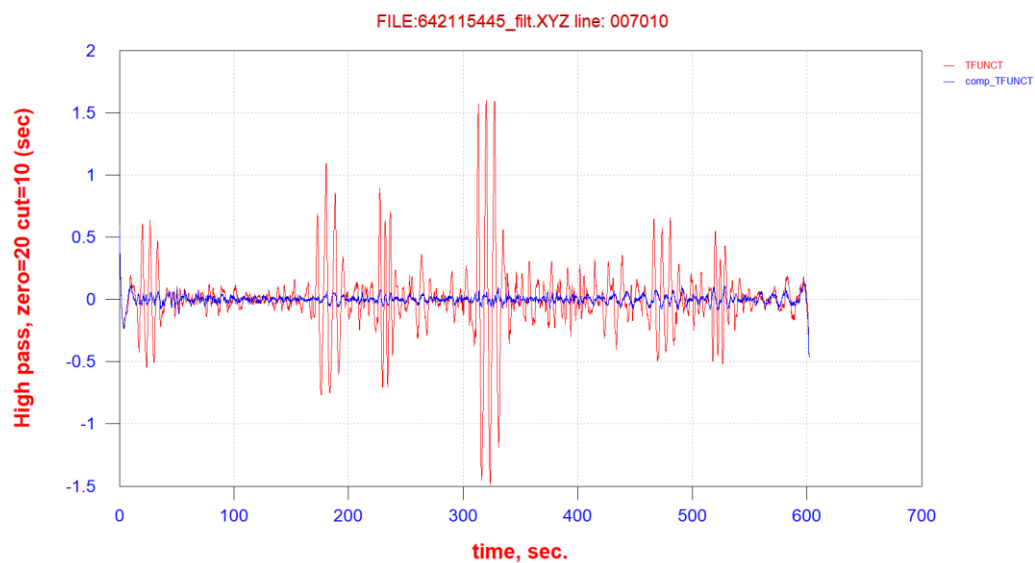
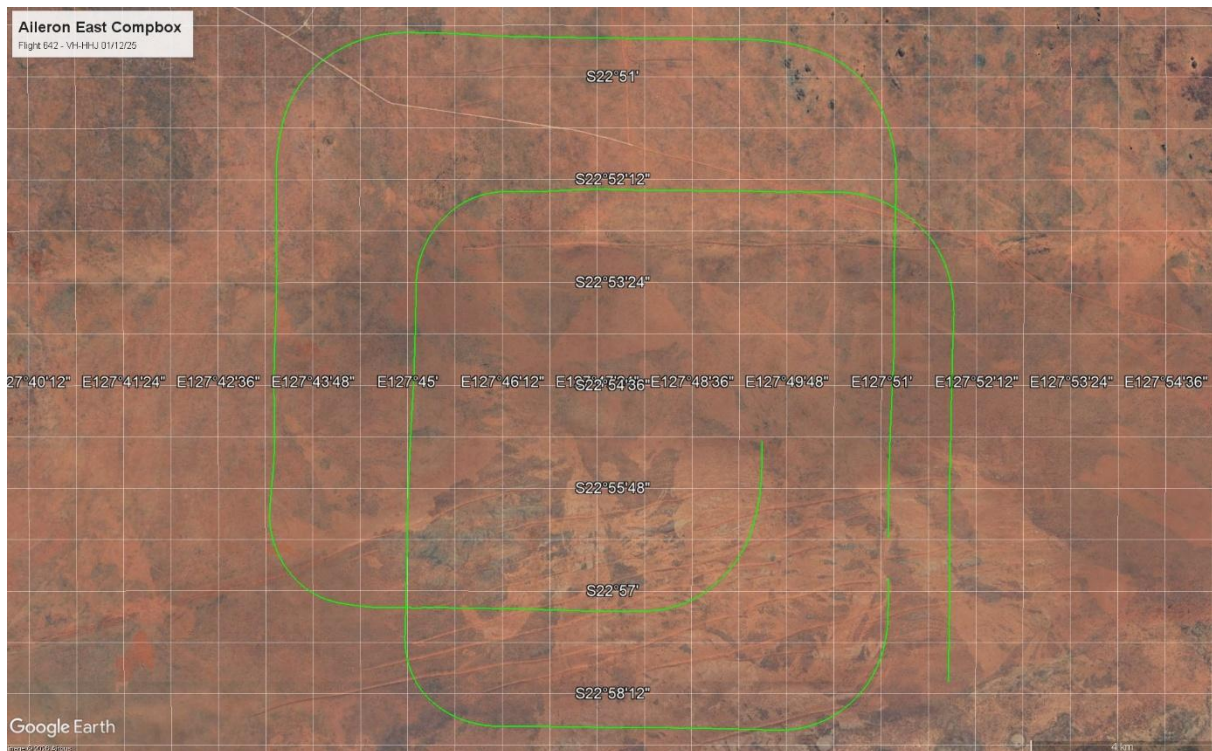


Compensation flight location (Google Earth)



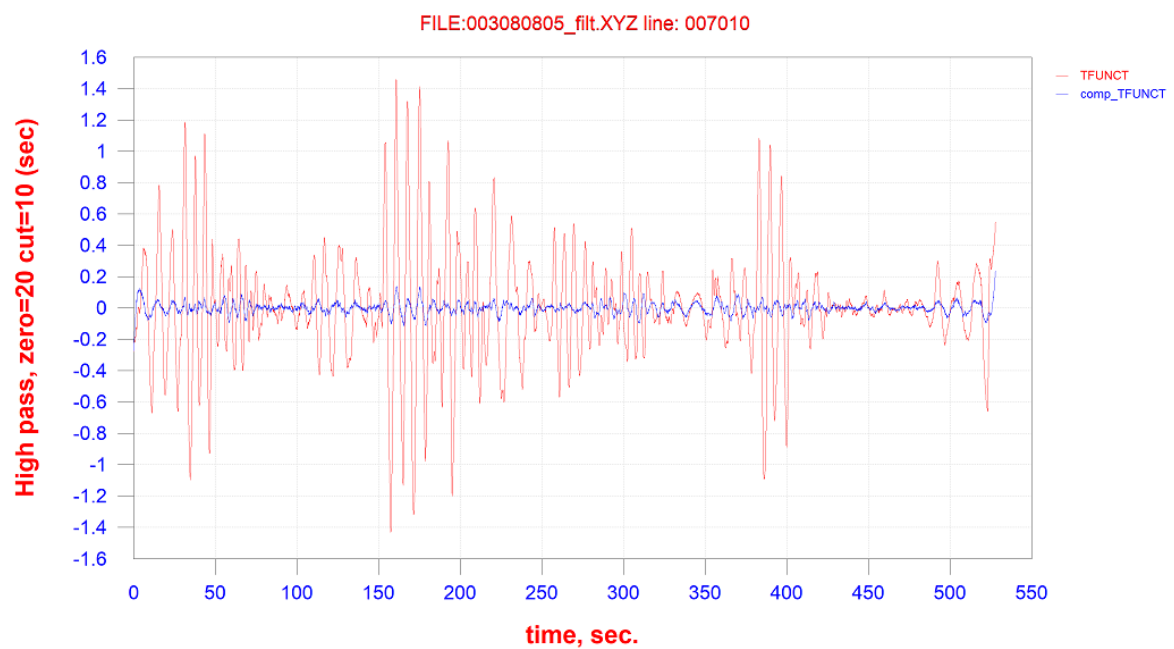
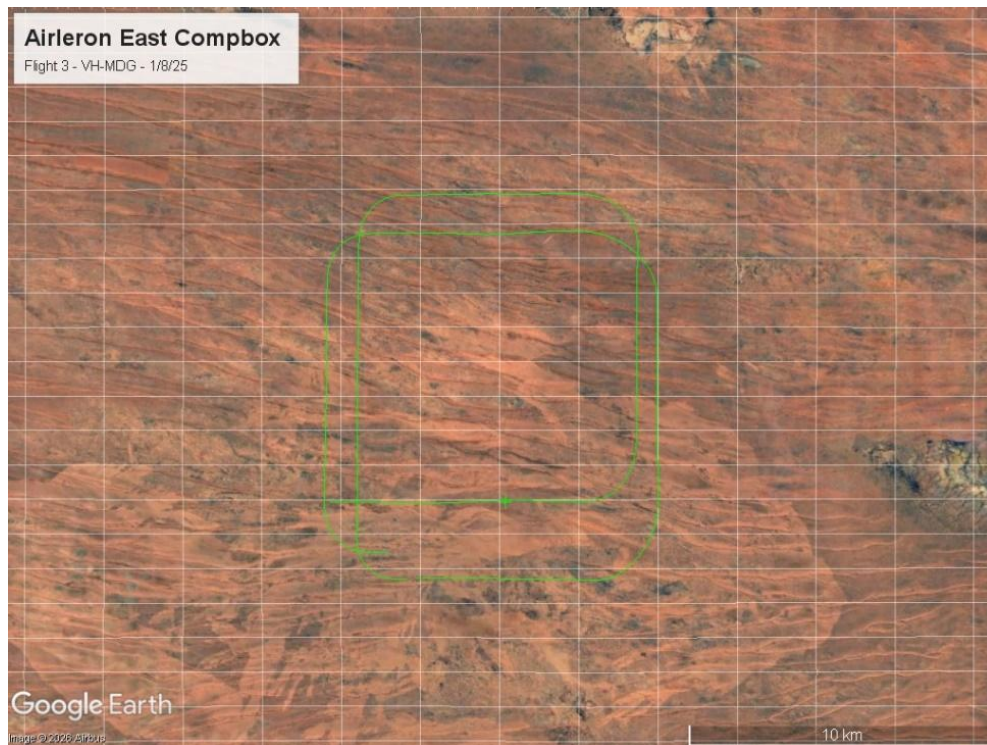
Sensor	Original RMS	Compensated RMS	Improvement Ratio
Tail	0.195	0.032	6.084

Processed Compensation Box Statistics

Magnetic Compensation Flight 642 (VH-HHJ) - 1st December 2025

Sensor	Original RMS	Compensated RMS	Improvement Ratio
Tail	0.263	0.030	8.839

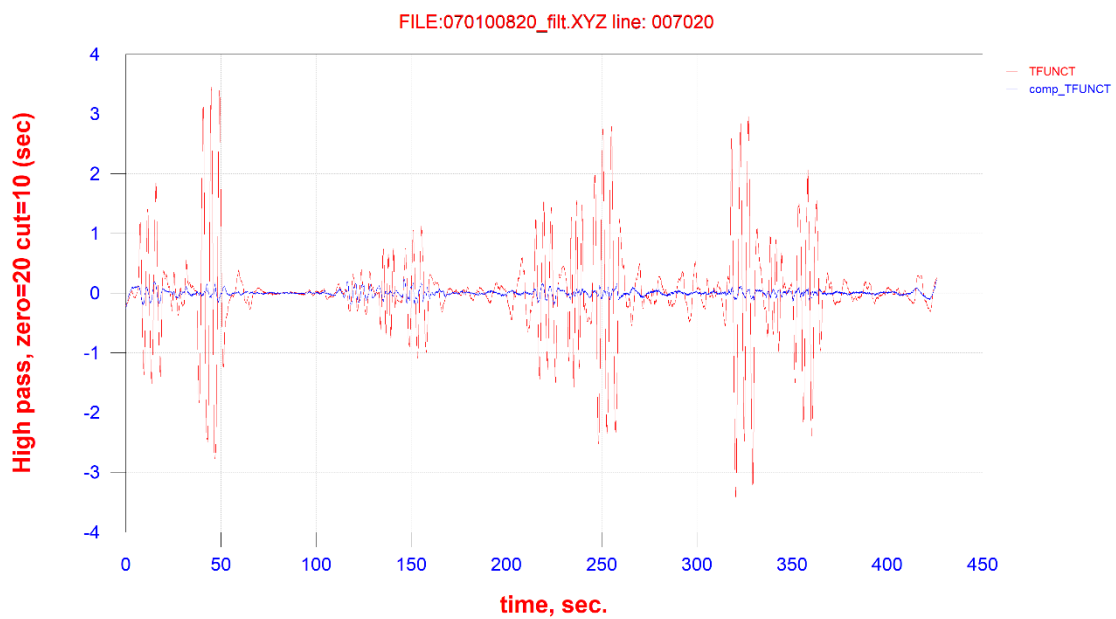
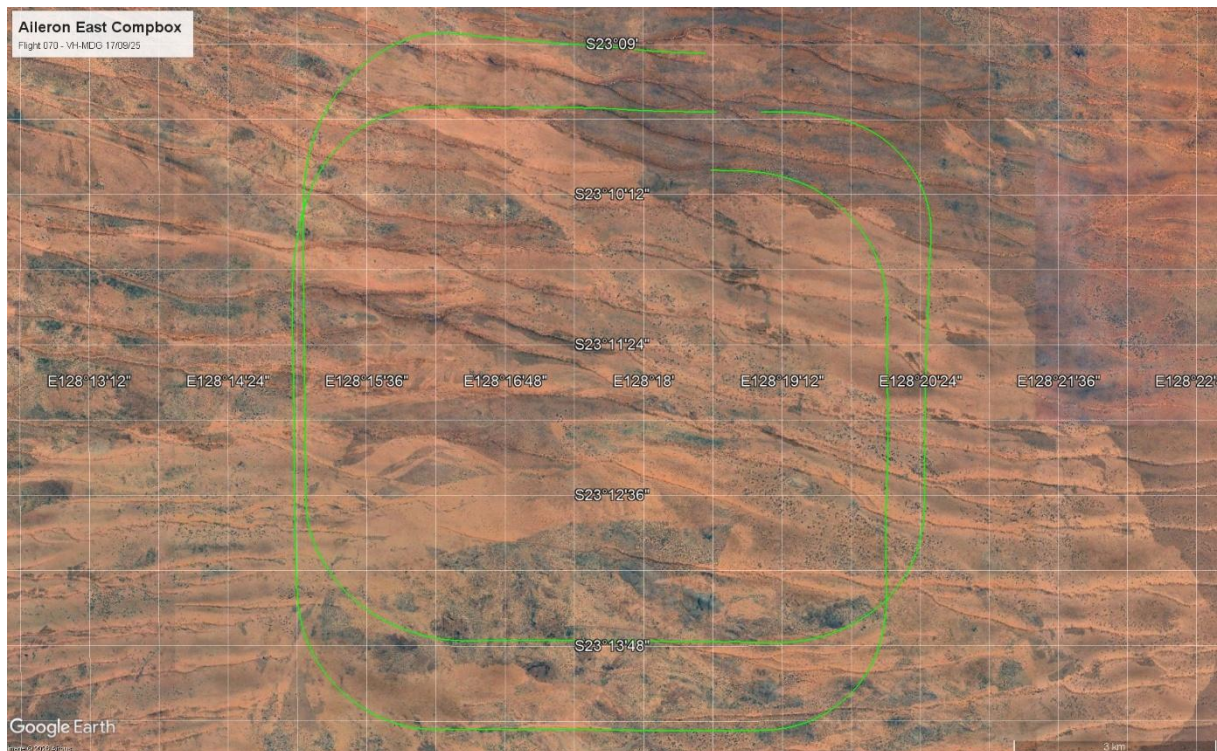
Processed Compensation Box Statistics

Magnetic Compensation Flight 3 (VH-MDG) - 1st August 2025

Sensor	Original RMS	Compensated RMS	Improvement Ratio
Tail	0.343	0.032	10.672

Processed Compensation Box Statistics

Magnetic Compensation Flight 070 (VH-MDG) – 17th September 2025



Sensor	Original RMS	Compensated RMS	Improvement Ratio
Tail	0.734	0.052	14.186

Processed Compensation Box Statistics

Base Station Magnetometers

The base station magnetometers were positioned near the Kiwirrkurra airstrip as shown below: -



Base Station Magnetometer Locations (Google Earth)

- Base station 1 location co-ordinates (GDA2020): -22.808747 ° S; 127.743668 ° E
- Base station 2 location co-ordinates (GDA2020): -22.808787 ° S; 127.744236 ° E

5 Magnetic Data Processing

The following steps were performed during the magnetics processing:

- Application of compensation
- Parallax correction
- Diurnal filtering and subtraction
- IGRF correction using the updated current IGRF model
- Tie line levelling
- Micro levelling

Compensation of the magnetometer data was applied using the recorded XYZ fluxgate data using Geometrics MagComp Airborne compensation software. The relevant compensation flight (comp box) was processed to obtain the optimum compensation solution which was then applied to the tail sensor data.

The base station magnetometer data were reviewed, de-spiked if necessary and filtered with an 11-point non-linear filter. These data were then subtracted from the survey data using time that was synchronised to both the acquisition system and the base mag unit. The base level used for reduction of the magnetic data was 53,670 nT.

The IGRF correction was applied using the IGRF 2025 model using a mean date of 2025.79 and adjusted for the height of the aircraft. This correction was calculated and applied at each point.

Tieline levelling was applied by way of a least-squares minimisation procedure using a polynomial fit of order 0 over the cross over errors calculated between the traverse and tie line intersections. A fit-to-ties process was selectively applied and constrained by several parameters such as cross over height differences and maximum and minimum allowable corrections.

Using MAGSPEC Airborne Surveys' proprietary micro levelling techniques, some selective micro levelling was carefully applied; and the resulting channel was then considered final.

The data were gridded with a cell size of 20 m, using a bi-cubic spline algorithm and delivered with projected coordinates.

Reduction to the Pole (RTP) was performed on the total magnetic intensity (TMI) grid.

At all stages of processing the data were stringently checked against and compared to the previous processing stage to ensure the integrity of the data were protected and no detail was removed or altered.

6 Radiometric Data Processing

Radiometric processing consisted of the following steps:

- 256-channel spectral noise reduction in the form of NASVD
- Dead time, cosmic and background radiation corrections
- Energy recalibration
- Channel interaction correction (stripping) and extraction of ROIs
- Height corrections using STP altitude to the nominal survey height
- Radon removal using the Spectral Ratio method
- Conversion to concentrations
- Levelling

The raw spectra were first smoothed using the Noise Adjusted Singular Value Decomposition (NASVD) method (Hovgaard and Grasty, 1997), on a full-dataset basis.

For the NASVD process twenty (20) principal components were generated. These components were visually inspected and the final number of components for reconstructing the spectra were determined. Eight (8) components were used to reconstruct the spectra (*refer to spectral component plots and difference images at the end of this section*).

For all spectrometers, spectral drift was checked, by monitoring the potassium and thorium channel positions from average spectra along flight lines. The procedure for determining peak positions was the same as used during calibration. If the thorium peak is found to move more than 1 channel or the potassium peak by more than 0.5 channel, energy calibration is performed to determine the count rates in the standard windows.

Both the aircraft 256-channel background spectra and the scaled 256-channel cosmic spectra were subtracted from the 256-channel data.

Deadtime corrections were applied to each spectrum channel or window.

Radon background removal was performed using the Minty Spectral Ratio method (1998).

In areas of significant topographic variation, the altimeter data were first lightly filtered to smooth sudden jumps that can arise when flying over steep terrain (which cause problems when height-correcting the data). These data were then converted to effective height at standard temperature and pressure (STP).

The background-corrected count rates in the three windows were stripped to give the counts in the potassium, uranium and thorium windows that originate solely from the potassium, uranium and thorium decay series. The window stripping ratios α , β , γ , a and g were estimated from measurements over calibration pads, where:

α - is the thorium into uranium stripping ratio, (equal to the ratio of counts detected in the uranium window to those detected in the thorium window from a pure thorium source);

β - is the thorium into potassium stripping ratio for a pure thorium source;

γ - is the uranium into potassium stripping ratio for a pure uranium source;

a - is the reversed stripping ratio, uranium into thorium, (equal to the ratio of counts detected in the thorium window to those detected in the uranium window from a pure source of uranium);

g - is the reverse stripping ratio, potassium into uranium for a pure potassium source.

The reverse stripping ratios a and g were not used because they have little effect on the stripped count rates in each window.

VH-MDG Stripping Ratios

Detector IDs	α	β	(γ)	a	g
5426 & 5489	0.3024	0.4723	0.7779	0.0261	0.0203
5489 & 6001	0.3045	0.4757	0.7763	0.0261	0.0117

VH-HHJ Stripping Ratios

Detector IDs	α	β	γ	a	g
6045 & 6046	0.3005	0.4869	0.7736	0.0289	0.0143

Each of the three main stripping ratios were adjusted for altitude before stripping was carried out, using the following values (Grasty and Minty 1995): -

Stripping Ratio	Increase per metre (IAEA 2003)
α	0.00049
β	0.00065
γ	0.00069

The background-corrected and stripped count rates were corrected for variations in the altitude of the detector using the following height attenuation coefficients (theoretical values used): -

	Total Count	Potassium	Uranium	Thorium
Height Attenuation Coefficient	0.0074	0.0094	0.0084	0.0074

The resulting potassium, uranium, thorium and total count (cps) were converted to concentrations using coefficients derived from the Carnamah (WA) radiometric test range.

Aircraft Call Sign	Total CPS / nGy/h	Potassium CPS / %	Uranium CPS / ppm	Thorium CPS / ppm
VH-MDG	33.5	110.3	9.2	6.4
VH-HHJ	33.6	108.1	10.1	6.4

Tieline levelling was applied to the channels to remove any residual effects. A least-squares/median filter procedure over the calculated cross over errors at each intersection of the flight and tie lines generated a correction value. A new tie-line levelled channel was then output by application of this correction value to the original channel.

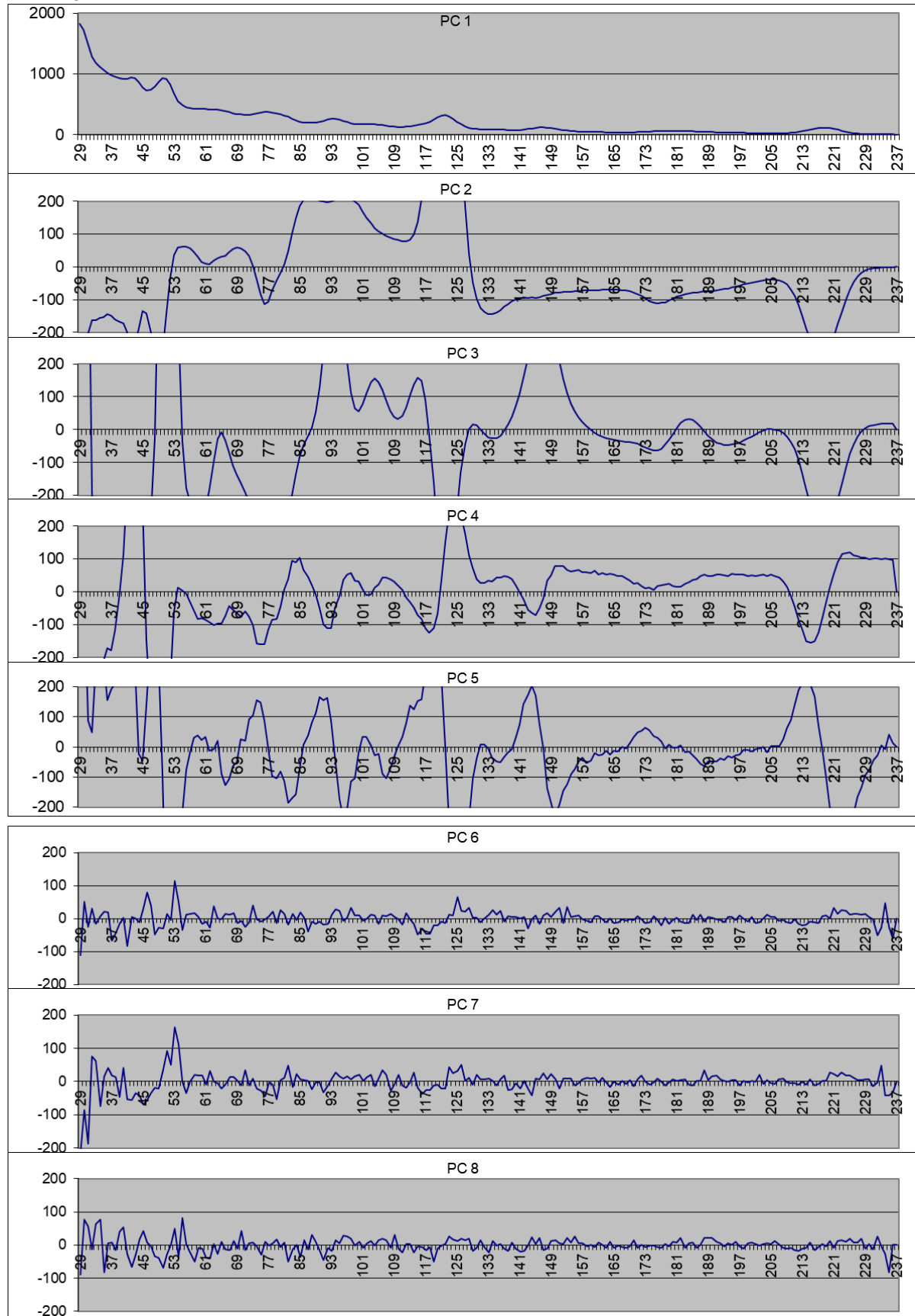
Where required, using MAGSPEC Airborne Surveys' proprietary micro levelling techniques, some selective micro levelling was carefully applied; and the resulting channels were then considered final.

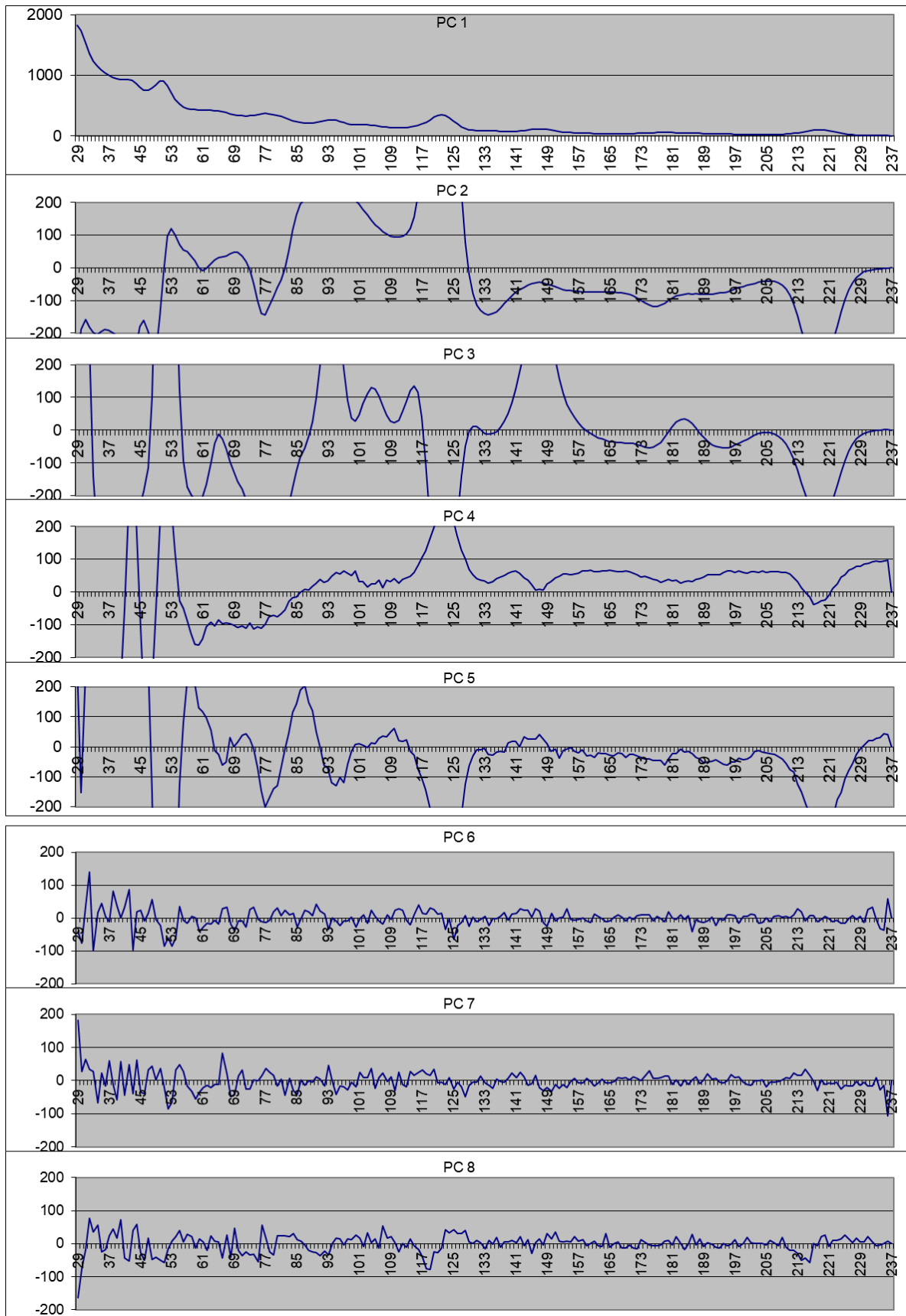
The data were gridded with a cell size of 20 m using a minimum curvature algorithm and delivered with projected coordinates.

At all stages of processing the data were stringently checked against and compared to the previous processing stage to ensure the integrity of the data was protected and no detail was removed or altered.

Spectral Data - Principal Components

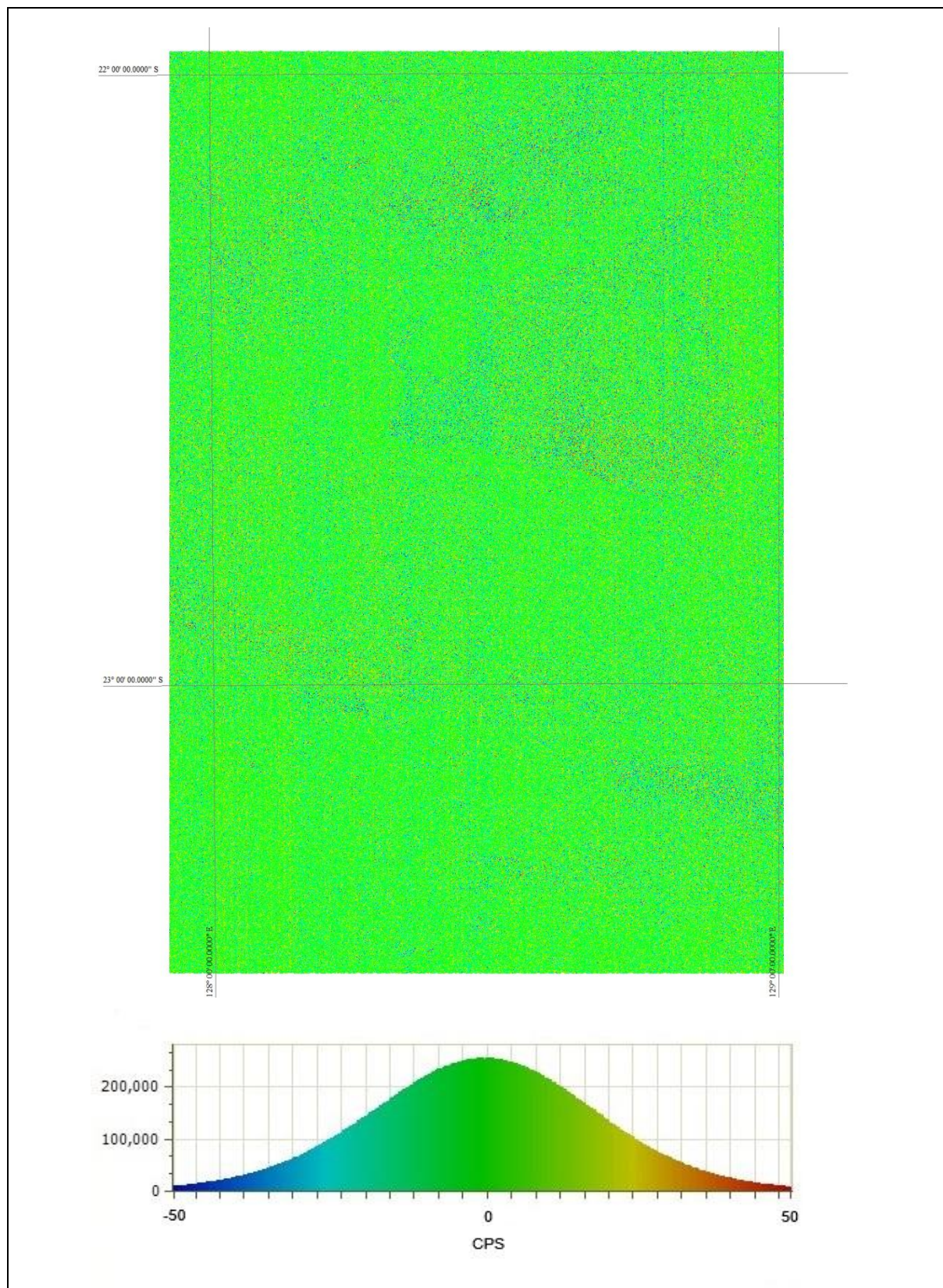
VH-HHJ



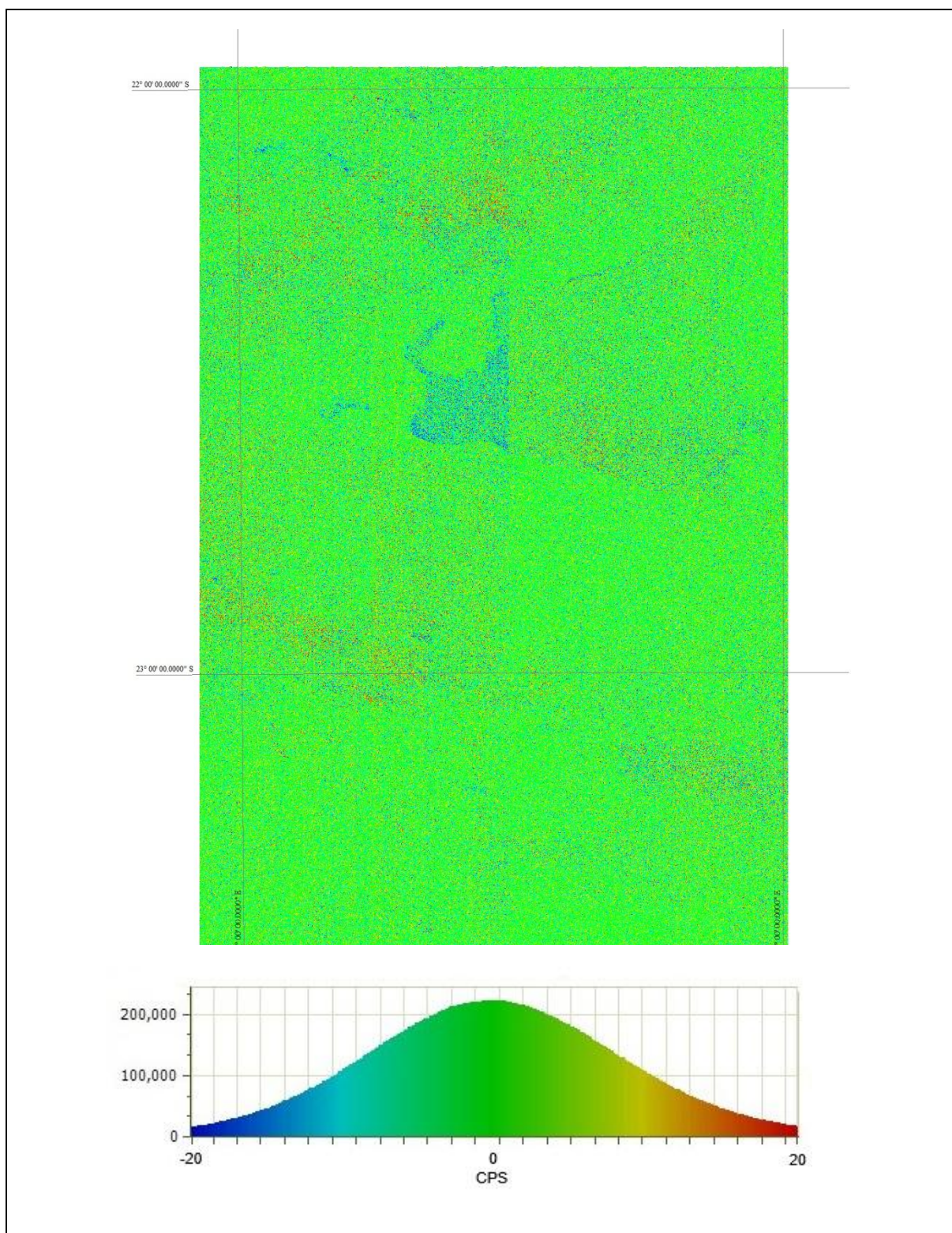
VH-MDG

NASVD Raw Window Counts

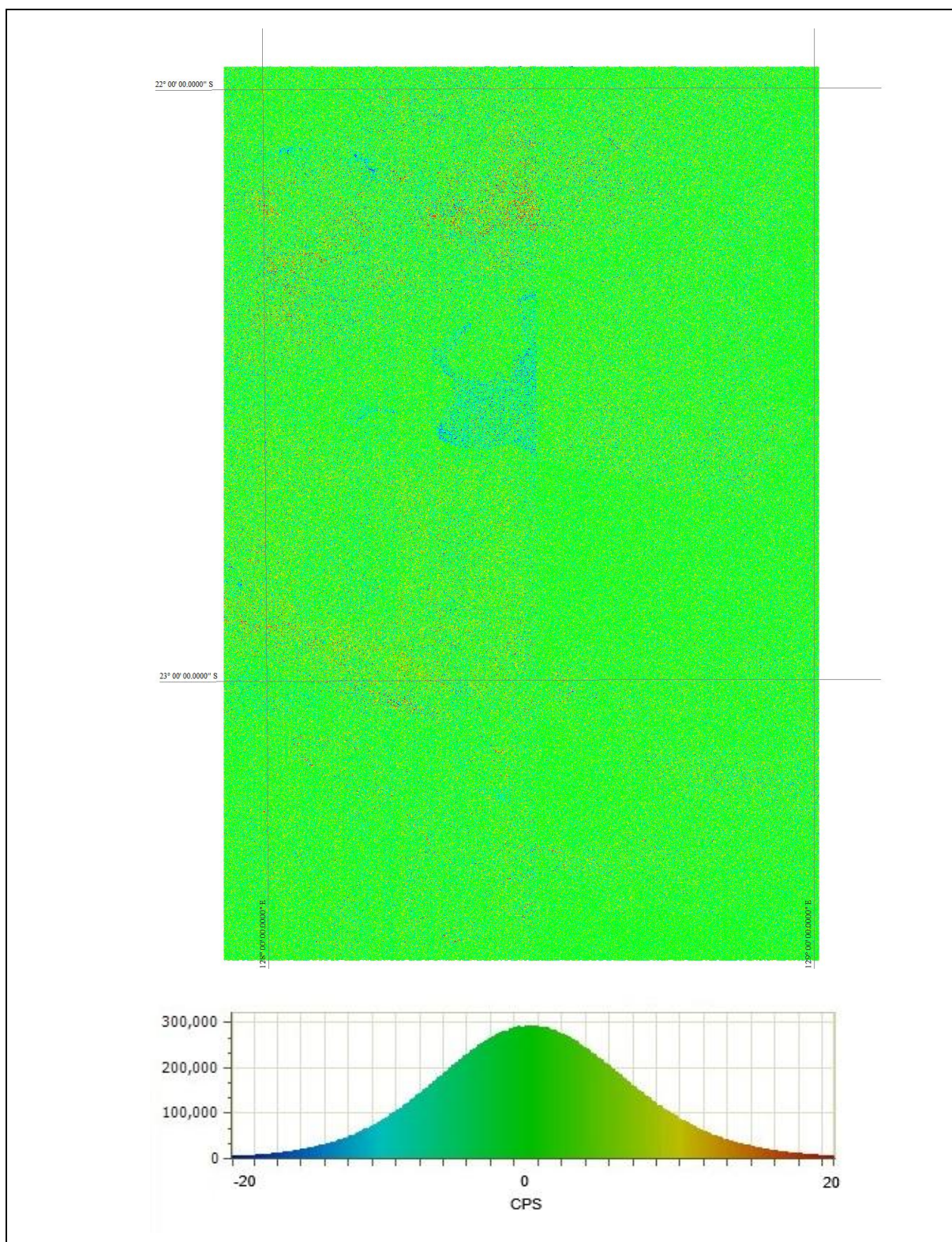
Difference images of pre- and post-NASVD raw window counts are displayed below.



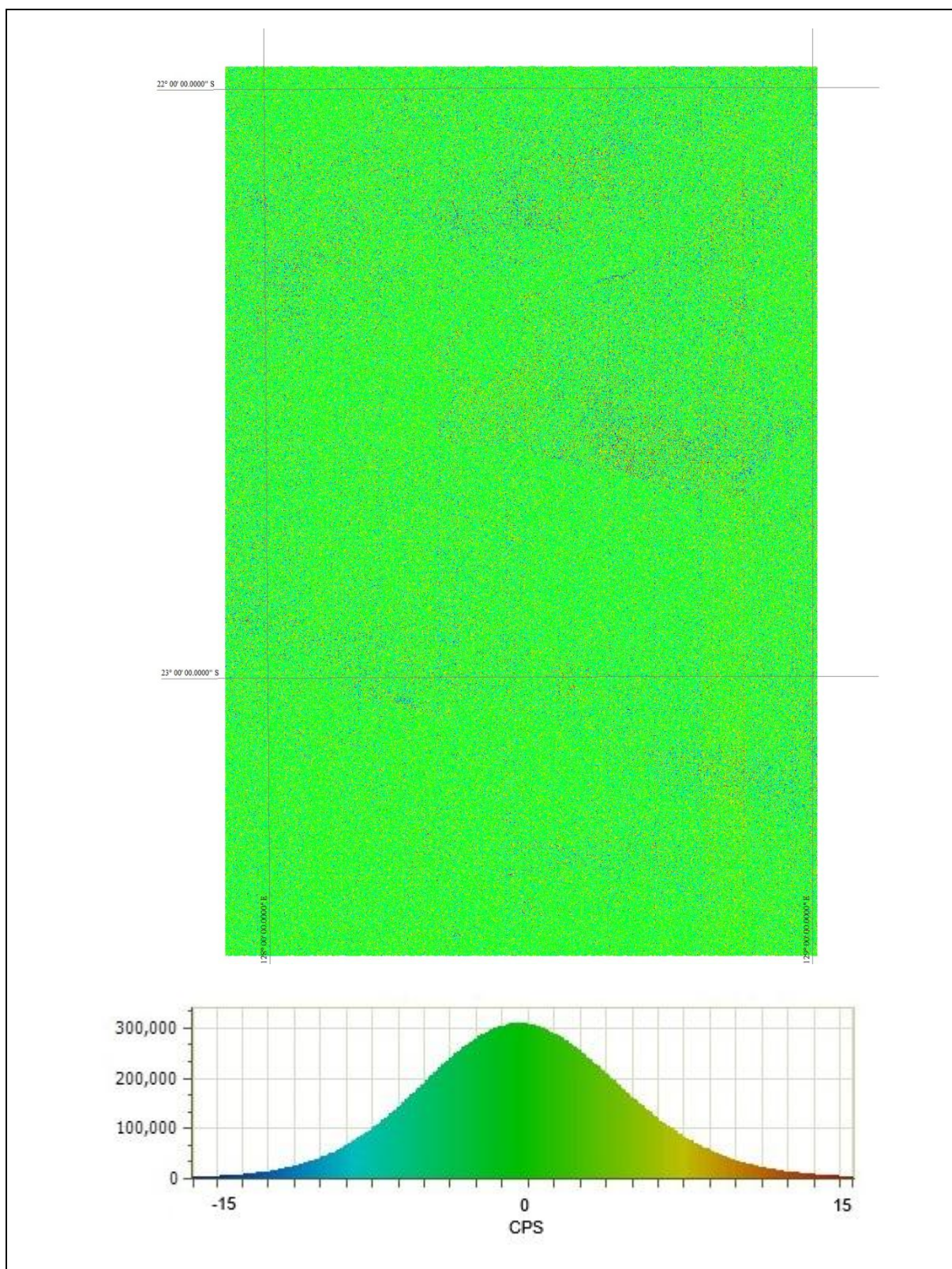
Total Count Difference



Potassium Count Difference



Raw Thorium Count Difference



Raw Uranium Count Difference

7 Elevation Data Processing

DEM processing consisted of the following steps:

- Inspection of height channels
- Parallax correction of radar altimeter
- Subtraction of radar altimeter from GPS height
- Tie line and micro levelling

The GPS and radar height data were visually inspected for errors, and any spikes were carefully corrected. The GPS ellipsoid height data were converted to the geoid height using the geoid-ellipsoid separation values from the Australian Vertical Working Surface (AVWS). The altimeter data were subtracted from the GPS height data to create the Digital Elevation channel.

Tieline levelling was applied by way of a least-squares minimisation procedure using a polynomial fit of order 0 over the cross over errors calculated between the traverse and tie line intersections. Using MAGSPEC Airborne Surveys' proprietary micro levelling techniques, some selective micro levelling was carefully applied; and the resulting channel was then considered final.

The data were gridded with a cell size of 20 m, using a minimum curvature algorithm and delivered with projected coordinates.

At all stages of processing the data were stringently checked against and compared to the previous processing stage to ensure the integrity of the data was protected and no detail was removed or altered.

8 File Names

The following is a list of digital files delivered.

+---IMAGES

```
| 20260210_DEMIRS24787_1_TMI_radar_DEM.tif
| 20260309_DEMIRS24787_1_TMI_reduced.tif
| 20260309_DEMIRS24787_1_TMI_reduced_RTP.tif
| 20260309_DEMIRS24787_1_TMI_reduced_RTP_1VD.tif
| 20260310_DEMIRS24787_1_Dose_Rate.tif
| 20260310_DEMIRS24787_1_K_concentration.tif
| 20260310_DEMIRS24787_1_Ternary.tif
| 20260310_DEMIRS24787_1_Th_concentration.tif
| 20260310_DEMIRS24787_1_U_concentration.tif
|
```

+---MAG

```
| +---DATA
| | \---ASCII
| | 20260309_DEMIRS24787_1_magnetics_reduced.DAT
| | 20260309_DEMIRS24787_1_magnetics_reduced.DES
| | 20260309_DEMIRS24787_1_magnetics_reduced.DFN
| |
```

| \---GRIDS

```
| 20260210_DEMIRS24787_1_TMI_radar_DEM
| 20260210_DEMIRS24787_1_TMI_radar_DEM.ers
| 20260309_DEMIRS24787_1_TMI_reduced
| 20260309_DEMIRS24787_1_TMI_reduced.ers
| 20260309_DEMIRS24787_1_TMI_reduced_RTP
| 20260309_DEMIRS24787_1_TMI_reduced_RTP.ers
| 20260309_DEMIRS24787_1_TMI_reduced_RTP_1VD
| 20260309_DEMIRS24787_1_TMI_reduced_RTP_1VD.ers
|
```

+---RAW_LOCATED

```
| | 20251215_DEMIRS24787_1_magnetics_raw_edited.dat
| | 20251215_DEMIRS24787_1_magnetics_raw_edited.DES
| | 20251215_DEMIRS24787_1_magnetics_raw_edited.DFN
| | 20251215_DEMIRS24787_1_magnetic_diurnal.dat
| | 20251215_DEMIRS24787_1_magnetic_diurnal.DES
| | 20251215_DEMIRS24787_1_magnetic_diurnal.DFN
| | 20251215_DEMIRS24787_1_Radiometrics_raw_edited.dat
| | 20251215_DEMIRS24787_1_Radiometrics_raw_edited.DES
| | 20251215_DEMIRS24787_1_Radiometrics_raw_edited.DFN
```

\---SPEC

+---DATA

```
| \---ASCII
| 20260310_DEMIRS24787_1_radiometrics_reduced.DAT
| 20260310_DEMIRS24787_1_radiometrics_reduced.DES
| 20260310_DEMIRS24787_1_radiometrics_reduced.DFN
|
```

\---GRIDS

20260310_DEMIRS24787_1_Dose_Rate
20260310_DEMIRS24787_1_Dose_Rate.ers
20260310_DEMIRS24787_1_K_concentration
20260310_DEMIRS24787_1_K_concentration.ers
20260310_DEMIRS24787_1_Th_concentration
20260310_DEMIRS24787_1_Th_concentration.ers
20260310_DEMIRS24787_1_U_concentration
20260310_DEMIRS24787_1_U_concentration.ers

9 Data Format

Separate point-located data files (.dat) were generated for the magnetic and radiometric data in ASEG-GDF2 format. The table below contains a description of the fields in each dataset.

Magnetics

Field Name	Format	Null Value	Unit	Description
Flight	I5	999		Flight number
Line	I9	9999999		Line number
FID	I9	9999999		Fiducial number
PSEUDO_LINE	I9	9999999		Pseudo Line
PSEUDO_FID	I9	9999999		Pseudo Fid
DATE	I10	99999999		YYYYMMDD Date
LONGITUDE	F13.7	999.9999999	degrees	GDA2020 Longitude
LATITUDE	F13.7	999.9999999	degrees	GDA2020 Latitude
EASTING	F11.2	999999.99	metres	GDA2020 MGA52 Easting
NORTHING	F12.2	9999999.99	metres	GDA2020 MGA52 Northing
GNSS_HEIGHT_GEIOD	F8.2	999.99	metres	Geoidal GPS Height
RADAR_CALIB_EDITED	F8.2	999.99	metres	Radar Altimeter (parallax corrected to location of Mag sensor, calibrated, edited & filtered)
RADAR_DEM	F8.2	999.99	metres	Geoidal surface derived Digital Elevation Model (DEM) derived from the radar altimeter
MAG_1_DIUR_IGRF	F11.3	99999.999	nT	Compensated edited corrected for diurnal variation and IGRF magnetics.
MAG_1_DIUR_IGRF_TIE	F11.3	99999.999	nT	Tie line levelled magnetics
MAG_1_DIUR_IGRF_TIE_MICRO	F11.3	99999.999	nT	Microlevelled magnetics
DIURNAL	F11.3	99999.999	nT	Magnetic Diurnal
IGRF	F11.3	99999.999	nT	IGRF (IGRF 2025 updated to 2025.79)

Radiometrics

Field Name	Format	Null Value	Unit	Description
Flight	I5	-999		Flight number
Line	I9	-9999999		Line number
FID	I9	-9999999		Fiducial number
PSEUDO_LINE	I9	-9999999		Pseudo Line
PSEUDO_FID	I9	-9999999		Pseudo Fid
DATE	I10	-99999999		YYYYMMDD Date
LONGITUDE	F13.7	-999.9999999	degrees	GDA2020 Longitude
LATITUDE	F13.7	-999.9999999	degrees	GDA2020 Latitude
EASTING	F11.2	-999999.99	metres	GDA2020 MGA52 Easting
NORTHING	F12.2	-9999999.99	metres	GDA2020 MGA52 Northing
GNSS_HEIGHT_GEOID	F8.2	-999.99	metres	GRS80 ellipsoidal GPS Height (edited & parallax corrected to location of half sample reading)
RADAR_CALIB_EDITED	F8.2	-999.99	metres	Radar Altimeter (parallax corrected, calibrated & edited)
RADAR_DEM	F8.2	-999.99	metres	Digital elevation model derived from the radar altimeter
PRESSURE	F8.2	-999.99	mbar	Baro pressure
TEMPERATURE	F7.2	-99.99	degrees C	Temperature
K_NASVD	F9.2	-999.99	cps	Raw NASVD K40 Counts
U_NASVD	F9.2	-999.99	cps	Raw NASVD Bi214 Counts
TH_NASVD	F9.2	-999.99	cps	Raw NASVD TI208 Counts
TOTAL_COUNT_NASVD	F11.3	-9999.999	cps	Raw NASVD Total Counts
K_NASVD_PROC	F9.2	-999.99	%	Corrected NASVD K40
U_NASVD_PROC	F9.2	-999.99	ppm	Corrected NASVD Bi214
TH_NASVD_PROC	F9.2	-999.99	ppm	Corrected NASVD TI208
DOSE_RATE_NASVD_PROC	F11.3	-9999.999	nGy/hr	Corrected NASVD Dose Rate
K_NASVD_PROC_TIE	F9.2	-999.99	%	Corrected Tie-Line Levelled NASVD K40
U_NASVD_PROC_TIE	F9.2	-999.99	ppm	Corrected Tie-Line Levelled NASVD Bi214
TH_NASVD_PROC_TIE	F9.2	-999.99	ppm	Corrected Tie-Line Levelled NASVD TI208
DOSE_RATE_NASVD_PROC_TIE	F11.3	-9999.999	nGy/hr	Corrected Tie-Line Levelled Dose rate
K_NASVD_PROC_TIE_MICRO	F9.2	-999.99	%	Corrected Tie-Line Levelled Micro-Levelled NASVD K40

U_NASVD_PROC_TIE_MICRO	F9.2	-999.99	ppm	Corrected Tie-Line Levelled Micro-Levelled NASVD Bi214
TH_NASVD_PROC_TIE_MICRO	F9.2	-999.99	ppm	Corrected Tie-Line Levelled Micro-Levelled NASVD TI208
DOSE_RATE_NASVD_PROC_TIE_MICRO	F11.3	-9999.999	nGy/hr	Corrected Tie-Line Levelled Micro-Levelled NASVD Dose Rate
RATIO_TH_K	F9.2	-999.99		Th/K Ratio
RATIO_U_K	F9.2	-999.99		U/K Ratio
RATIO_TH_U	F9.2	-999.99		Th/U Ratio

10 Images of Grids

GeoTIFF (.tif) images of the above grids were generated at 600 dpi.

All images were generated using Geosoft Oasis Montaj and enhanced with equal area distribution, sun angles at 45 degree elevation and 45 degree azimuth. The colour tables used were as follows: -

- TMIs and RTPs: rainbow1.lut
- Vertical Derivatives: greyscale.lut
- Radiometrics: pseudocolour.lut
- Ternary Radiometrics (K, Th,U): red.tbl, green.tbl, blue.tbl

11 Quality Control Summary

Survey statistics are compiled from the Daily and Weekly Report information for each aircraft and are included in a separate Appendix:

- *DEMIRS24787_1436_AileronEast_OperationsProcessing_Report_Appendix.pdf*

This Appendix includes the following tables and plots: -

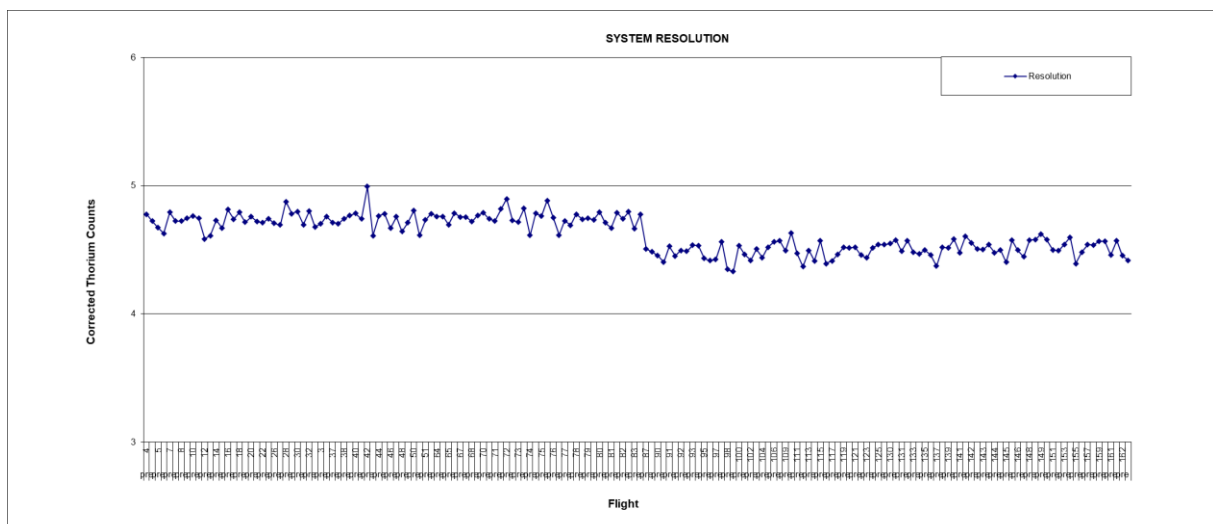
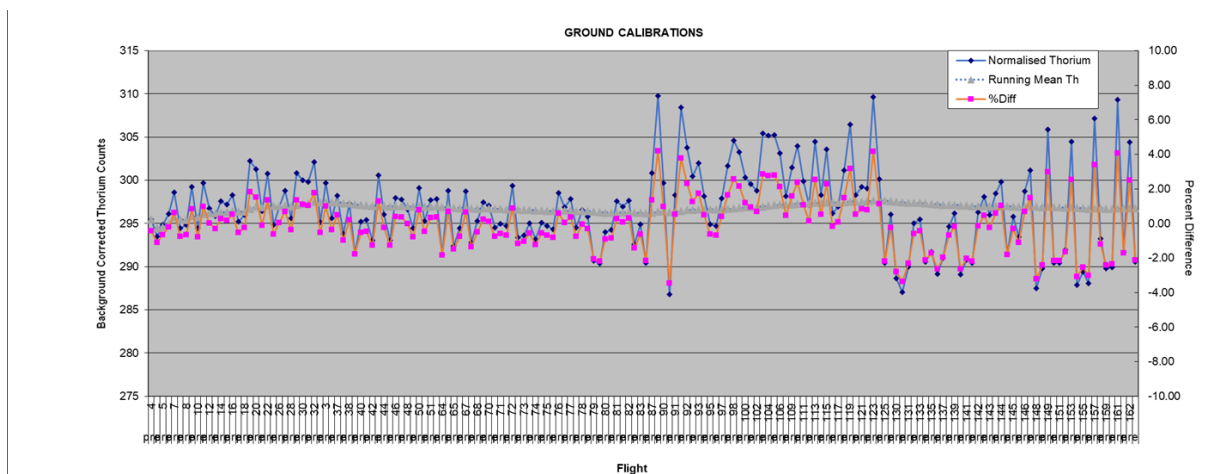
1. GNSS accuracy summary

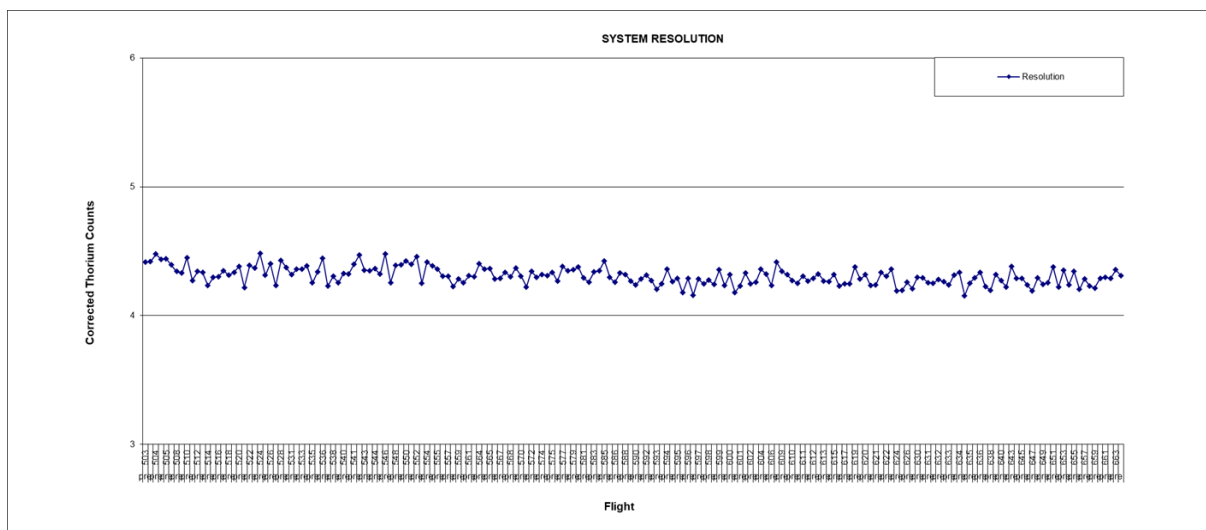
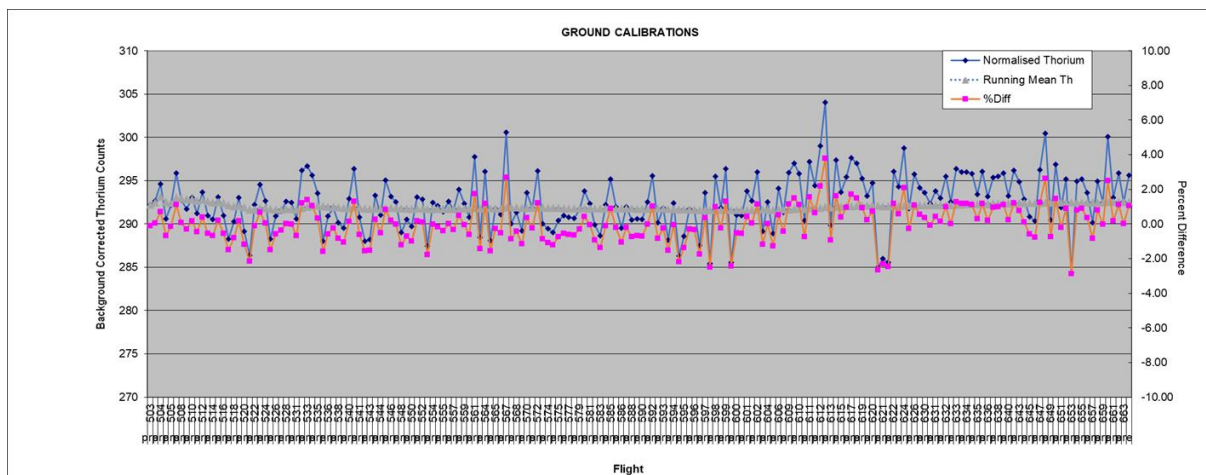
- tables of the positional accuracy of the Global Navigation Satellite System for each aircraft.

2. Daily Thorium Source Checks

- tables of the thorium and background counts and system resolution for each flight and aircraft. These tables are summarised by the following plots:-

VH-MDG

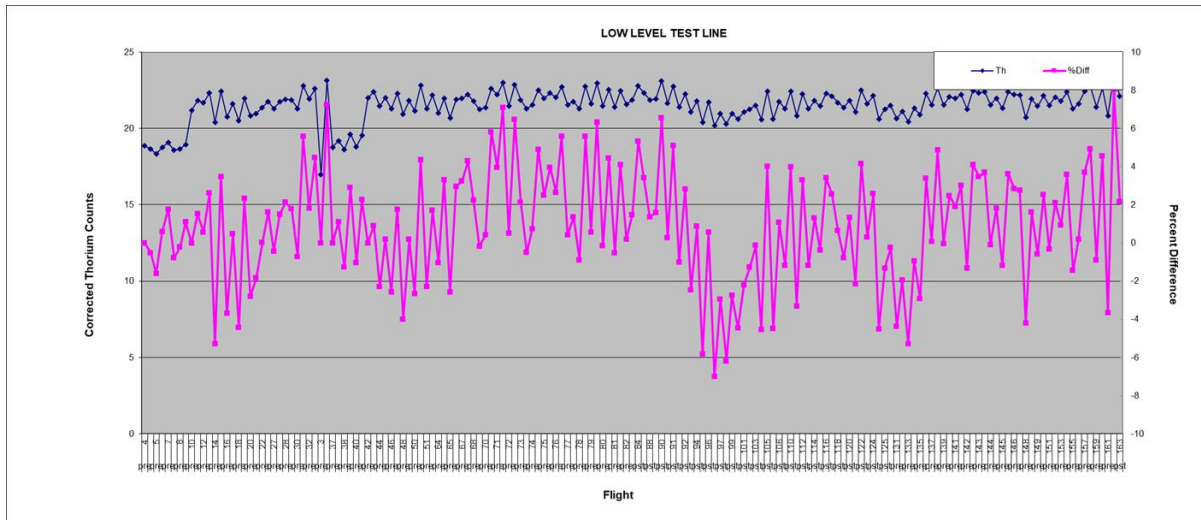


VH-HHJ

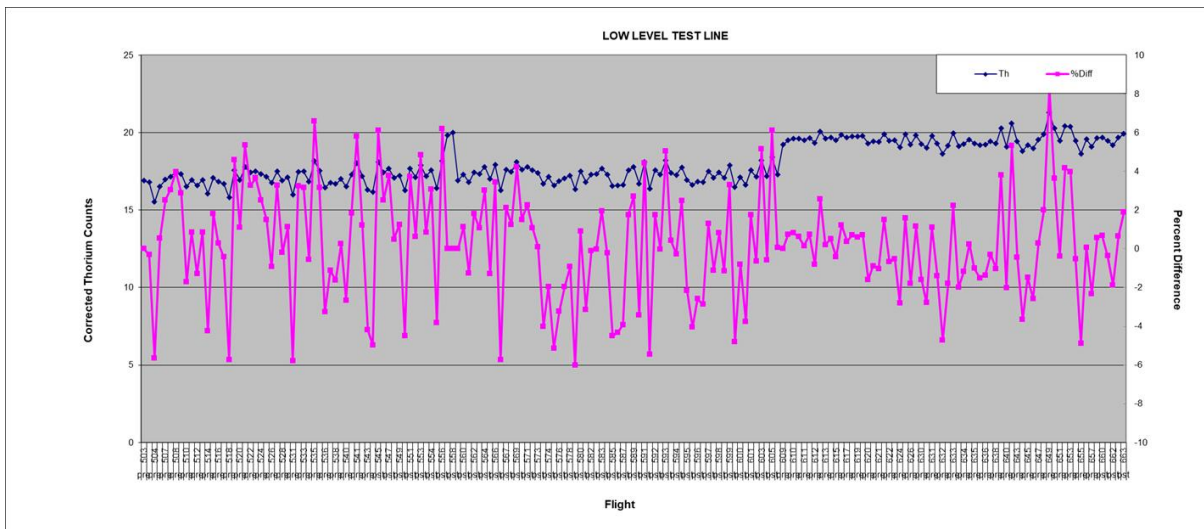
3. Low Level Test Line Summary

- tables of the average thorium count from the survey test lines for each flight and aircraft.
These tables are summarised by the following plots:-

VH-MDG



VH-HHJ



4. Flight Logs

- summary of each flight, including line kilometres flown and any occurrence of standby.

5. Weather / Temperature

- description of daily weather including temperature, wind, rainfall and diurnal activity.

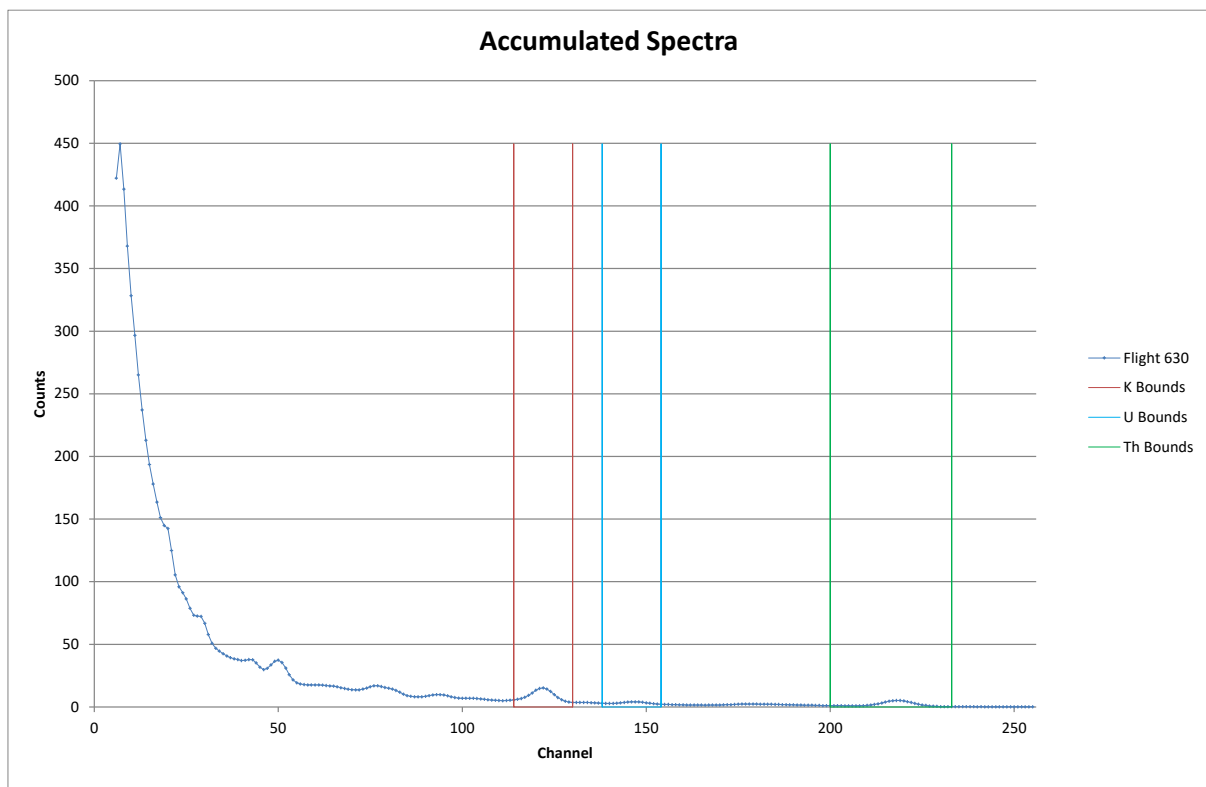
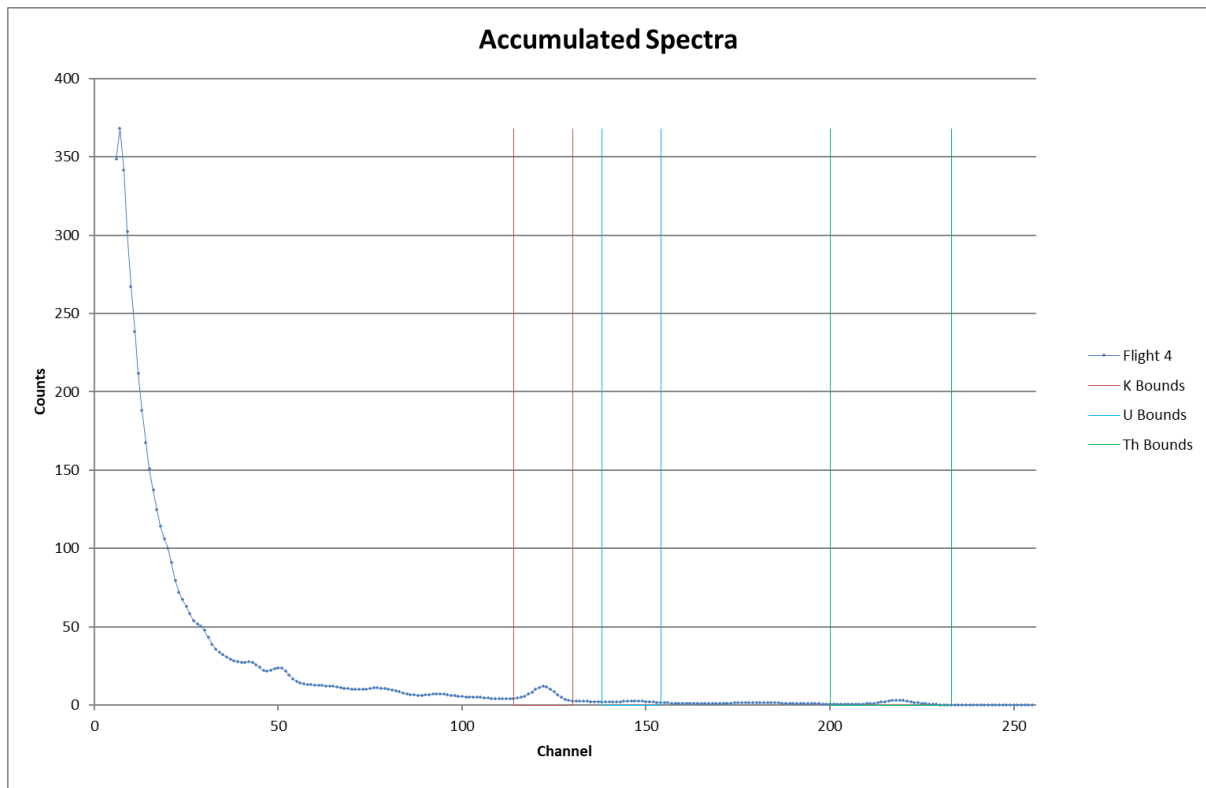
6. Reflight List

- a table of survey lines that were partially (P) reflight or scrubbed (S), due to departures from the specifications; as shown below: -

Line No.	Kms	Flight No.	Date	P/S	Reflight No.	Reflight Date	Reason
106660	167.01	626	8/11/2025	S	661	14/12/2025	Diurnal
106710	167.01	573	19/09/2025	P	614	30/10/2025	System
107190	167.01	626	8/11/2025	S	661	14/12/2025	Diurnal
107200	167.01	626	8/11/2025	S	661	14/12/2025	Diurnal
108150	167.01	603	18/10/2025	P	613	30/10/2025	Diurnal
108160	167.01	603	18/10/2025	S	661	14/12/2025	Diurnal
110320	167.01	528	16/08/2025	P	535	21/08/2025	System
101430	167.01	67	15/09/2025	S	83	7/10/2025	Diurnal
104390	167.01	119	8/11/2025	S	161	6/12/2025	Diurnal
104410	167.01	131	16/11/2025	S	131	16/11/2025	Water in Lake

7. Radiometric Spectrum Plots

- plots of accumulated gamma-ray spectra (the average intensity (cps) vs. channel number) for each aircraft and flight. Example plots are shown below: -



12 References

Hovgaard, J., and Grasty, R.L., 1997. *Reducing statistical noise in airborne gamma ray data through spectral component analysis*. In "Proceedings of Exploration 97: Fourth Decennial Conference on Mineral Exploration" edited by A.G.Gubins, 1997, 753-764.

Grasty, R.L. and Minty B.R.S., 1995. *A guide to the technical specifications for airborne gamma-ray surveys*. AGSO Record 1995/60.

IAEA, 2003. *Guidelines for radioelement mapping using gamma-ray spectrometry data*, IAEA-TECDOC-1363, International Atomic Energy Agency, Vienna (2003).

Minty, B.R.S., 1998. *Multichannel models for the estimation of radon background in airborne gamma-ray spectrometry*. Geophysics, 63(6), 1986–1996.